

COMPRESSION OF USER GENERATED CONTENT USING DENOISED REFERENCES

Eduardo Pavez*, Enrique Perez*, Xin Xiong*, Antonio Ortega*, Balu Adsumilli†

*University of Southern California, Los Angeles, California, USA

†Google Inc, Mountain View, CA

ABSTRACT

Video shared over the internet is commonly referred to as user generated content (UGC). UGC video may have low quality due to various factors including previous compression. UGC video is uploaded by users, and then it is re encoded to be made available at various levels of quality and resolution. In a traditional video coding pipeline the encoder parameters are optimized to minimize a rate-distortion criteria, but when the input signal has low quality, this results in sub-optimal coding parameters optimized to preserve undesirable artifacts. In this paper we formulate the UGC compression problem as that of compression of a noisy/corrupted source. The noisy source coding theorem reveals that an optimal UGC compression system is comprised of optimal denoising of the UGC signal, followed by compression of the denoised signal. Since optimal denoising is unattainable and users may be against modification of their content, we propose using denoised references to compute distortion, so the encoding process can be guided towards perceptually better solutions. We demonstrate the effectiveness of the proposed strategy for JPEG compression of UGC images and videos.

Index Terms— user generated content, noisy source coding, video compression, alternative reference metric, denoising

1. INTRODUCTION

Video sharing applications (e.g., YouTube, TikTok) produce a large percentage of Internet traffic. This type of video is commonly referred to as user generated content (UGC) [1]. UGC is first uploaded by users and then it is re-encoded by service providers in order to be made available at various levels of quality and resolution. The traditional video compression pipeline assumes the input video is pristine, however this is often not true for UGC, where the source material has been compressed by the users sharing it. In addition, UGC may have low quality due to additional factors, e.g., use of non professional video equipment, poor shooting skills, low light, editing, special effects, etc.

In the traditional video compression pipeline, the encoder/decoder parameters are optimized to minimize the distortion, subject to bitrate (and additional computational complexity) constraints [2, 3]. However, when the distortion is computed with respect to a corrupted reference signal, the rate distortion optimization process may lead to suboptimal coding parameters that preserve undesirable features that do not lead to improved perceptual quality (e.g., blocking artifacts due to previous compression).

The fundamental UGC compression problem is to, *given an UGC signal and a compression system (e.g., JPEG, AVI), choose*

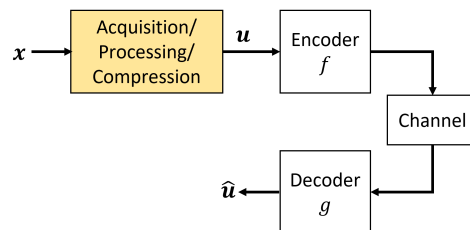


Fig. 1: Block diagram for UGC video coding. x is the pristine (unknown) signal, u is the UGC video, and \hat{u} is the reconstructed signal at the decoder.

coding parameters, to accurately represent and encode the perceptually meaningful parts of the signal, while avoiding allocating resources to encode compression artifacts and noise.

To address the issue of a low quality and unreliable reference, researchers have proposed using non reference metrics to assess subjective video quality [4, 5], which can be used to perceptually optimize (guide) the compression of UGC videos. Another approach classifies UGC based on content category and similarity in rate-distortion characteristics, so that fixed coding parameters can be used for each UGC class [6, 7]. While previous works have recognized that the encoding process should adapt to the quality of the input UGC video, and have provided tools and insights to design UGC compression systems, we take a step towards solving the UGC compression problem from a rate-distortion theoretic perspective [8]. In Section 2 we formulate the UGC compression problem as an instance of noisy source coding, where the noiseless source corresponds to the pristine original, and the noisy/corrupted signal is the UGC. This process is depicted in Figure 1. In this ideal scenario, the goal is to minimize distortion computed with respect to the pristine (unknown) original. By invoking a noisy source coding theorem, we can show that the optimal encoder-decoder system in the mean-squared-error (MSE) sense is comprised of optimal MSE estimation of the clean source from the noisy source, followed by optimal (noiseless) source coding of this estimate [9, 10, 8]. The noisy source coding theorem has been applied to compression of noisy images [11], speech coding [12, 13, 14] and to the design of video coding systems robust to pre- and post-processing [15, 16]. However, to the best of our knowledge, it has not been applied yet to UGC compression.

Note that in traditional video coding the distortion goes to zero as the rate increases and the quality of the encoded video improves. In contrast, a consequence of the noisy source coding theorem is that distortion with respect to the UGC source should not go to zero, i.e., further increases in bitrate beyond a certain point do not lead to improved performance. This is because in the UGC coding scenario, we wish to minimize distortion with respect to the pristine reference,

This work was funded in part by a gift from YouTube. Author's email: {pavezcar, perezern, xiongxin, aortega}@usc.edu

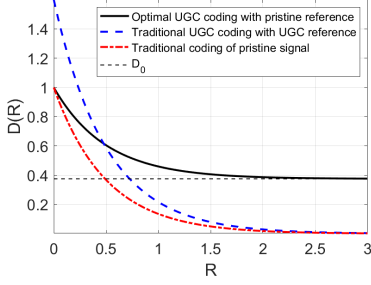


Fig. 2: Optimal distortion-rate functions for scalar zero mean Gaussian sources. Comparison of optimal RD curves for: encoding x with reference x , encoding of noisy signal $u = x + \eta$, with u as reference ($D(R)$ from (1)), and encoding of u with pristine source x as original ($D^{\text{ugc}}(R)$ from (3)). x has variance $\sigma_x^2 = 1$, the UGC signal is $u = x + \eta$, where η is a zero mean Gaussian with variance $\sigma_\eta^2 = 0.6$, independent of x .

but we have to do this without being able to encode the pristine signal directly. An example of the optimal rate-distortion curve for a Gaussian source corrupted by additive Gaussian noise [10] is depicted in Figure 2. When distortion is computed with respect to the noisy input, the distortion quickly goes to zero, while for the optimal UGC coding system, distortion decreases more slowly and saturates to a positive distortion value.

While encoding a denoised signal is theoretically optimal, in a practical system it may be preferable to encode the UGC signal directly instead, because: 1) users may object to a service provider modifying their uploaded content, and 2) finding good denoising/restoration algorithms may be difficult, given that there may be multiple reasons for quality degradation in a UGC signal and thus a specific denoiser may not always produce reliable outputs. Hence, we propose to use a denoised UGC signal only as a proxy to compute distortion, i.e., as a replacement for the (unavailable) pristine original, while using the UGC signal itself as the source for the encoder. In Section 3 we show experimentally that the rate-distortion curve of this system has a saturation region, similar to the optimal RD curve. We use this and propose an algorithm to choose coding parameters based on detecting saturation of the distortion curve, to avoid encoding a bitrates for which the encoded signal quality does not improve. We show that for a JPEG encoder, the quality parameter associated with the onset of the saturation region, is positively correlated with the perceptual quality of the UGC video.

2. THE UGC COMPRESSION PROBLEM

In this section we propose a theoretical formulation of the UGC compression problem. We show that optimal denoising is essential for efficient compression of UGC. We then propose a practical framework using an off-the shelf denoiser to guide the encoder towards a reference signal that approximates the optimal denoised reference.

2.1. Noisy source coding

In the UGC compression problem (Figure 1) \mathbf{x} and \mathbf{u} are random vectors representing the pristine content and the UGC signal, respectively. The encoded representation is denoted by $b = f(\mathbf{u})$, where f is the encoder, while the number of bits of the representation b is denoted by $\ell(b)$. The output of the decoder is denoted by

$\hat{\mathbf{u}} = g(f(\mathbf{u}))$. For a given rate R , a traditional (noiseless) source coding problem has the form

$$D(R) = \min_{f,g} \mathbb{E}[\|\mathbf{u} - \hat{\mathbf{u}}\|^2] \text{ s.t. } \ell(f(\mathbf{u})) \leq R, \quad (1)$$

where $D(R)$ is the distortion rate function. Note that as the bitrate R increases in (1), $\hat{\mathbf{u}} \rightarrow \mathbf{u}$ and the distortion $D(R)$ decreases so that $\lim_{R \rightarrow \infty} D(R) = 0$. This is problematic, because at high rates low distortion simply means that \mathbf{u} and $\hat{\mathbf{u}}$ are close, but the best possible representation (\mathbf{u} , corresponding to $D(R) = 0$) is not guaranteed to have good quality, given that the input \mathbf{u} is UGC.

Ideally, since the source is noisy, the source coding problem should be formulated so that distortion is computed with respect to the pristine original:

$$D^{\text{ugc}}(R) = \min_{f,g} \mathbb{E}[\|\mathbf{x} - \hat{\mathbf{u}}\|^2] \text{ s.t. } \ell(f(\mathbf{u})) \leq R. \quad (2)$$

Under the optimality criterion of (2) the decoded signal $\hat{\mathbf{u}}$ has to approximate the pristine content \mathbf{x} . The following result allows us to break down (2) into two simpler steps: 1) optimal denoising, and 2) optimal (noiseless) source coding.

Theorem 1. [9, 10, 8] *The optimal distortion-rate function for the UGC coding problem is:*

$$D^{\text{ugc}}(R) = D_0 + \min_{f,g} \mathbb{E}[\|\mathbf{y} - \hat{\mathbf{u}}\|^2] \text{ s.t. } \ell(\bar{f}(\mathbf{y})) \leq R, \quad (3)$$

where $D_0 = \mathbb{E}[\|\mathbf{x} - \mathbf{y}\|^2]$, $\mathbf{y} = \mathbb{E}[\mathbf{x} | \mathbf{u}]$, and $\hat{\mathbf{u}} = \bar{g}(\bar{f}(\mathbf{y}))$.

Note that \mathbf{y} is the minimum mean square error estimator (MMSEE) of the pristine signal, which does not depend on the encoder/decoder functions, or the rate R . The proof of Theorem 1 [9, 10, 8] uses two facts: (i) \mathbf{y} and $(f \circ g)(\mathbf{y})$ are measurable functions of \mathbf{u} and (ii) the MMSEE is orthogonal, namely $\mathbb{E}[(\mathbf{x} - \mathbf{y})h(\mathbf{u})] = 0$, for any measurable function h .

A first consequence of Theorem 1 is the lower bound

$$D^{\text{ugc}}(R) \geq D_0, \quad (4)$$

which establishes that D_0 is the lowest achievable distortion by any encoder/decoder, at any rate. Since D_0 is the error of the MMSEE, it can be interpreted as a quality metric of the UGC signal. Another consequence of Theorem 1 is that for an encoder/decoder to asymptotically achieve this lower bound, that is, $\lim_{R \rightarrow \infty} D^{\text{ugc}}(R) = D_0$, we have that $f = \bar{f} \circ \text{MMSEE}$, while $g = \bar{g}$ is the corresponding decoder for \bar{f} . In other words, an optimal UGC compression system has two components:

1. Optimal denoising with the MMSEE, $\mathbf{y} = \mathbb{E}[\mathbf{x} | \mathbf{u}]$,
2. Lossy encoding/decoding that acts on \mathbf{y} instead of \mathbf{u} .

Example optimal distortion-rate curves are shown in Figure 2, where we consider a zero mean scalar Gaussian source x , contaminated with additive independent zero mean Gaussian noise η . For this example, we can compare the derivatives of $D(R)$ from (1) and $D^{\text{ugc}}(R)$ from (3) using formulas from [10] to obtain

$$\left| \frac{\partial D^{\text{ugc}}(R)}{\partial R} \right| = \left(\frac{\text{var}(x)}{\text{var}(u)} \right)^2 \left| \frac{\partial D(R)}{\partial R} \right| \leq \left| \frac{\partial D(R)}{\partial R} \right|, \quad (5)$$

where we used $\text{var}(x)/\text{var}(u) = \text{var}(x)/(\text{var}(x) + \text{var}(\eta)) \leq 1$. Therefore, the formulation (i.e., (1)), suggests that by increasing the rate by 1 bit, quality improves by $|\partial D(R)/\partial R|$, while in fact a correct formulation (i.e., (3)) only guarantees the more modest improvement by $|\partial D^{\text{ugc}}(R)/\partial R|$.

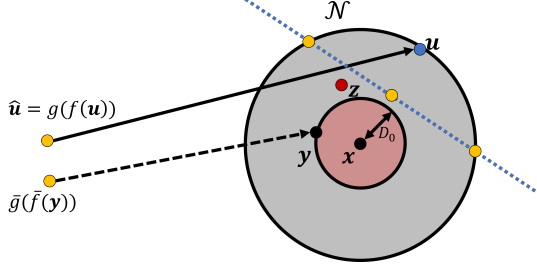


Fig. 3: UGC encoding strategies using difference signals for encoder input and reference metric.

While [Theorem 1](#) gives us a clear solution, its implementation is impractical for several reasons. First, optimal MSE denoising depends on the signal \mathbf{x} , and on the joint distribution of \mathbf{x} and \mathbf{u} , which are unknown. Second, while practical video codecs can achieve impressive compression performance using rate-distortion optimization of encoding parameters for a single video [2, 3], the noisy source coding formulation (3) is concerned with guaranteeing optimality in an average sense, i.e., when considering the average performance for a family of signals \mathbf{u} , \mathbf{x} with the same distribution. Third, while [Theorem 1](#) suggests directly encoding a denoised signal \mathbf{y} , this may be undesirable for the reasons mentioned in the introduction (users may not want their content to be modified and the denoising/estimation methods may not be reliable).

2.2. UGC compression with denoised references

We propose compressing the UGC signal \mathbf{u} using the signal $\mathbf{z} = \mathcal{D}(\mathbf{u})$ as a reference for distortion computation, where $\mathcal{D}(\cdot)$ is a denoiser. Using this metric we can guide the encoding process towards solutions with fewer artifacts. The main idea behind our proposal is illustrated in [Figure 3](#). According to the noise source coding theory, points inside the red circle with \mathbf{x} at the center will have distortions that are not achievable. The MMSEE \mathbf{y} is a point in the boundary of that red circle and thus ideal UGC compression using \mathbf{x} as reference is depicted by the dashed arrow, where as the bitrate increases, the encoded signal $\bar{g}(\bar{f}(\mathbf{y}))$ approaches \mathbf{y} . A standard UGC encoder is represented by a solid black arrow, such that as the bitrate increases the encoded signal $\hat{\mathbf{u}} = g(f(\mathbf{u}))$ approaches \mathbf{u} . Note that when the bitrate R is small, $\hat{\mathbf{u}}$ is at similar distance from both the UGC signal and the pristine original, that is $\|\hat{\mathbf{u}} - \mathbf{x}\| \approx \|\hat{\mathbf{u}} - \mathbf{u}\| \gg \|\mathbf{u} - \mathbf{x}\|$, thus in this regime, an encoded version of \mathbf{u} may look similar to an encoded version of \mathbf{x} . In this figure we can see that as the rate increases $\hat{\mathbf{u}}$ will become closer to \mathbf{u} at the expense of increasing the distance to \mathbf{x} , which would be clearly undesirable. Thus, we can define a *noise encoding region*, corresponding to the family of all encoder/decoders (with their parameters), for which the encoded signal $\hat{\mathbf{u}}$ is closer to \mathbf{u} than \mathbf{x} , or more precisely

$$\mathcal{N} = \{(f, g) : \|g(f(\mathbf{u})) - \mathbf{x}\| > \|g(f(\mathbf{u})) - \mathbf{u}\|\}. \quad (6)$$

The boundary of the noise encoding region is depicted by a blue dashed line in [Figure 3](#). Our goal is to avoid \mathcal{N} , and find encoder/decoder pairs, $(f, g) \notin \mathcal{N}$. Clearly, \mathcal{N} cannot be found, given that we do not have access to \mathbf{x} . If the denoised signal is a better approximation to the pristine original than the UGC signal, that is, $\|\mathbf{z} - \mathbf{x}\| < \|\mathbf{u} - \mathbf{x}\|$, then we can use \mathbf{z} to guide $\hat{\mathbf{u}}$ away for \mathbf{u} as the rate R increases. Thus, we propose to define an *empirical noise*

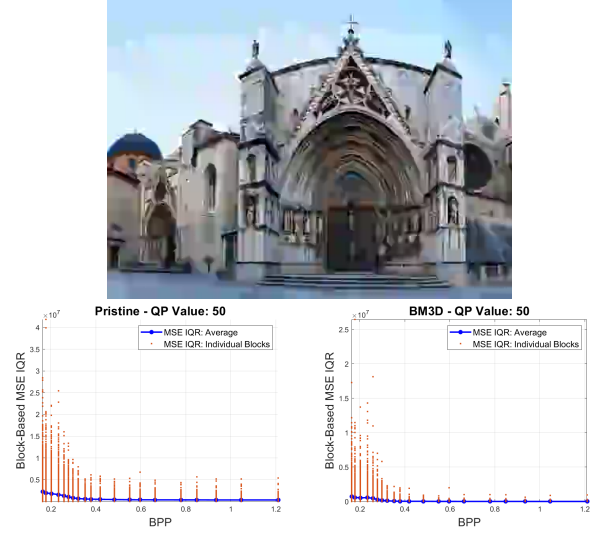


Fig. 4: MSE values for individual blocks and their IQR. Synthetic UGC image created by compression with H.264 using quantization parameter $QP = 45$ (top). Block MSE with respect to pristine original (left), and block MSE with respect to BM3D denoised reference (right).

encoding region using the denoised reference,

$$\mathcal{N}_{\mathcal{D}} = \{(f, g) : \|g(f(\mathbf{u})) - \mathcal{D}(\mathbf{u})\| > \|g(f(\mathbf{u})) - \mathbf{u}\|\}, \quad (7)$$

which can be used to choose coding parameters.

3. EXPERIMENTS

To find the region in which the distortion saturates and the quality of the UGC signal does not improve (see [Figure 2](#)), we use denoised reference signals and the criteria to detect $\mathcal{N}_{\mathcal{D}}$ from (7). For simplicity, our experiments use JPEG for compression. Within a single image, different regions have varying levels of complexity and correspondingly require different bitrates to achieve the same quality. Since different images will have different mixes of high and low complexity blocks, we do not use the overall MSE and instead we partition each image into $k \times k$ blocks and use the per-block MSEs to detect saturation of the distortion function. Specifically, to capture the typical block behaviour and to remove outliers, we use the Interquartile Range (IQR) of the per-block MSE. Letting E_i be the MSE from the i th block (for either pristine reference or denoised reference), and assuming that the E_i are sorted by magnitude, so that $E_i \leq E_{i+1}$ for all blocks, the MSE IQR is defined as

$$\text{MSE-IQR} = E_{i_2} - E_{i_1}, \quad (8)$$

where E_{i_1} is larger than 25% of the values, and E_{i_2} is larger than 75% of the values. The MSE-IQR captures the variation of the middle 50% of the block MSE values, while removing outliers.

3.1. Experiments with synthetic UGC images

In this section we show experimentally that when the UGC has low quality due to previous compression, RD curves computed using the pristine original and the denoised UGC content have a similar saturation region. We used pristine images from the KADID-10k dataset

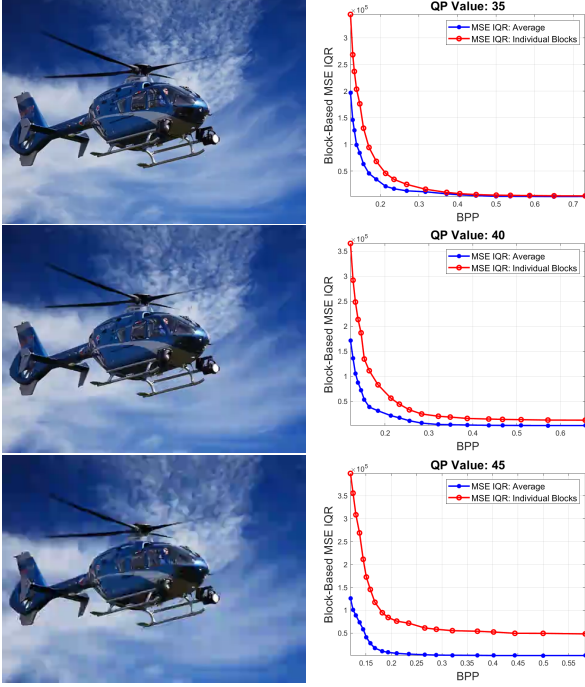


Fig. 5: Synthetic UGC images obtained by H.264 compression with high quality (top-left $QP = 35$), intermediate quality (middle-left, $QP = 40$), and low quality (bottom-left, $QP = 45$). Saturation of block-based MSE-IQR curves (right).

[17], and compressed them with H.264. In Figure 4, we depict an example of a heavily compressed image to be used as UGC. This UGC image is then encoded with JPEG at 20 different bitrates. For each bitrate, the image is divided into 8×8 blocks, and for each block we compute MSE with respect to the pristine original and with respect to a *BM3D* denoised [18] reference. Figure 4 also shows the per block MSE as a function of the total bitrate. At lower bitrate, there is high variation of MSE across blocks, while for higher bitrates, this variation decreases. In Figure 5 we plot the MSE-IQR computed for pristine and denoised references, as a function of the bitrate. For the same UGC image, with different levels of quality, we observe that the both distortions, pristine and alternative references, saturate at similar bitrates, which decrease with the UGC quality level.

3.2. Experiments with YouTube UGC dataset

YouTube UGC is a large scale dataset sampled from Youtube videos. Each video clip in YouTube UGC is accompanied by a mean-opinion-score (MOS) that provides a subjective measure of their quality. Videos are also annotated with 15 different content type categories. The dataset provides users with two versions of original videos: RAW YUV and almost lossless compressed videos using H264 CRF 10. We use the H264 CRF 10 versions. For each clip we sample 10 frames, starting from the 15th frame, and sampling every 30 frames. The denoised references are computed using the Python Scikit-Image [19] implementation of the *BayesShrink* wavelet denoiser [20]. We encode each frame with JPEG (using the Pillow Python implementation [21]), using 20 different quality values ($QV_n, n = 1, \dots, 20$). The QV_n ranges from 14 (worst) to 90 (best) with interval 4. Our goal is to find a saturation quality value QV^* , so that if we chose a QV_n larger than QV^* (i.e., we increase

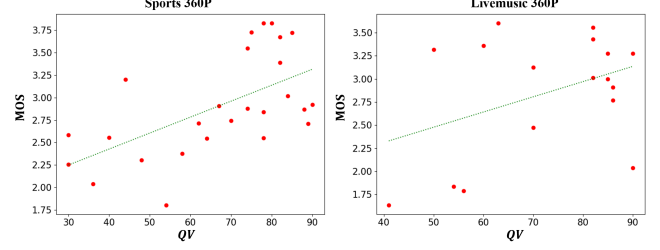


Fig. 6: Scatter plot of MOS and saturation quality value QV^* . Each point represent a video clip from Youtube UGC.

the bitrate), the quality of the encoded UGC has saturated. Let $\mathbf{u}_{i,t}$ and $\mathbf{z}_{i,t}$ denote the i th blocks of the t th frames of the UGC, and denoised UGC signals, respectively, while $\hat{\mathbf{u}}_{i,t,n}$ is the i th block, of the t th frame of the UGC encoded using QV_n . Applying the saturation criteria (7) to each block, we compute

$$\delta_{t,n,i} = \begin{cases} 1 & \text{if } \|\hat{\mathbf{u}}_{i,t,n} - \mathbf{u}_{i,t}\| \leq \|\hat{\mathbf{u}}_{i,t,n} - \mathbf{z}_{i,t}\| \\ 0 & \text{otherwise} \end{cases} \quad (9)$$

We say that the i th block of the t th frame has saturated at quality value QV_n if $\delta_{t,n,i} = 1$. We define the saturation quality value $QV_{i,t}^* = QV_{n^*}$ for the i th block in frame t , as the smallest quality value, that satisfies, for all $n \geq n^*$

$$QV_{i,t}^* = QV_{n^*} \leq QV_n, \text{ and } \delta_{t,n,i} = 1. \quad (10)$$

If $\delta_{t,n,i} = 0$ for all n , then we say that the block does not saturate and $QV_{i,t}^* = \max_n QV_n$. The saturation quality value of the frame t is computed as $QV_t^* = \text{median}(\{QV_{i,t}^*\}_i)$. The saturation quality value of the clip is computed as $QV^* = \text{median}(\{QV_t^*\}_t)$. Video clips from the Sport and Livemusic categories with resolution 360P are used to show the correlation between MOS and saturation QV^* , where the MOS value used is measured for the first 10 seconds rather than the whole video. In Figure 6, we observe positive correlation between MOS and QV^* . Note that a perceptual metric such as MOS depends on multiple factors, including the content quality, and not just the compression quality of the UGC content. Thus, while we do observe positive correlation it is not surprising that correlation is not perfect.

4. CONCLUSION

We have formulated the problem of compression of user generated content (UGC), as compression of a noisy/distorted source. Using classic results from rate-distortion theory, we showed that optimal UGC compression can be obtained by optimal denoising/restoration followed by optimal compression of a noiseless signal. Since in practical systems, it may be undesirable and challenging to find good denoising/restoration algorithms, we propose instead, using a denoised reference to compute distortion, and guide (regularize) the compression process, to avoid spending bitrate in encoding noise and undesirable artifacts. We perform experiments on synthetic UGC images, and show that distortion-rate curves with denoised UGC as a reference, shares similar saturation properties as the distortion-rate curve that uses the pristine (unknown) signal as reference. We then propose a simple method to detect distortion saturation of YouTube UGC videos, and demonstrate that the Quality Parameter of a JPEG encoder, at which the distortion saturates, is positively correlated with the mean-opinion-score.

5. REFERENCES

- [1] Yilin Wang, Sasi Inguva, and Balu Adsumilli, "YouTube UGC dataset for video compression research," in *2019 IEEE 21st International Workshop on Multimedia Signal Processing (MMSP)*. IEEE, 2019, pp. 1–5.
- [2] Antonio Ortega and Kannan Ramchandran, "Rate-distortion methods for image and video compression," *IEEE Signal processing magazine*, vol. 15, no. 6, pp. 23–50, 1998.
- [3] Gary J Sullivan and Thomas Wiegand, "Rate-distortion optimization for video compression," *IEEE signal processing magazine*, vol. 15, no. 6, pp. 74–90, 1998.
- [4] Xiangxu Yu, Neil Birkbeck, Yilin Wang, Christos G Bampis, Balu Adsumilli, and Alan C Bovik, "Predicting the quality of compressed videos with pre-existing distortions," *IEEE Transactions on Image Processing*, vol. 30, pp. 7511–7526, 2021.
- [5] Anish Mittal, Anush Krishna Moorthy, and Alan Conrad Bovik, "No-reference image quality assessment in the spatial domain," *IEEE Transactions on image processing*, vol. 21, no. 12, pp. 4695–4708, 2012.
- [6] Sam John, Akshay Gadde, and Balu Adsumilli, "Rate distortion optimization over large scale video corpus with machine learning," in *2020 IEEE International Conference on Image Processing (ICIP)*. IEEE, 2020, pp. 1286–1290.
- [7] Suiyi Ling, Yoann Baveye, Patrick Le Callet, Jim Skinner, and Ioannis Katsavounidis, "Towards perceptually-optimized compression of user generated content (UGC): Prediction of UGC rate-distortion category," in *2020 IEEE International Conference on Multimedia and Expo (ICME)*. IEEE, 2020, pp. 1–6.
- [8] T. Berger, *Rate Distortion Theory: A Mathematical Basis for Data Compression*, Prentice-Hall electrical engineering series. Prentice-Hall, 1971.
- [9] R. Dobrushin and B. Tsybakov, "Information transmission with additional noise," *IRE Transactions on Information Theory*, vol. 8, no. 5, pp. 293–304, 1962.
- [10] J Wolf and Jacob Ziv, "Transmission of noisy information to a noisy receiver with minimum distortion," *IEEE Transactions on Information Theory*, vol. 16, no. 4, pp. 406–411, 1970.
- [11] Osama K Al-Shaykh and Russell M Mersereau, "Lossy compression of noisy images," *IEEE Transactions on Image Processing*, vol. 7, no. 12, pp. 1641–1652, 1998.
- [12] Yariv Ephraim and Robert M. Gray, "A unified approach for encoding clean and noisy sources by means of waveform and autoregressive model vector quantization," *IEEE Transactions on Information Theory*, vol. 34, no. 4, pp. 826–834, 1988.
- [13] Thomas R Fischer, Jerry D Gibson, and Boneung Koo, "Estimation and noisy source coding," *IEEE Transactions on Acoustics, Speech, and Signal Processing*, vol. 38, no. 1, pp. 23–34, 1990.
- [14] JD Gibson, B Koo, and SD Gray, "Filtering of colored noise for speech enhancement and coding," *IEEE Transactions on Signal Processing*, vol. 39, no. 8, pp. 1732–1742, 1991.
- [15] Yehuda Dar, Alfred M Bruckstein, Michael Elad, and Raja Giryes, "Postprocessing of compressed images via sequential denoising," *IEEE Transactions on Image Processing*, vol. 25, no. 7, pp. 3044–3058, 2016.
- [16] Yehuda Dar, Michael Elad, and Alfred M Bruckstein, "Optimized pre-compensating compression," *IEEE Transactions on Image Processing*, vol. 27, no. 10, pp. 4798–4809, 2018.
- [17] Hanhe Lin, Vlad Hosu, and Dietmar Saupe, "Kadid-10k: A large-scale artificially distorted iqa database," in *2019 Tenth International Conference on Quality of Multimedia Experience (QoMEX)*. IEEE, 2019, pp. 1–3.
- [18] Ymir Mäkinen, Lucio Azzari, and Alessandro Foi, "Collaborative filtering of correlated noise: Exact transform-domain variance for improved shrinkage and patch matching," *IEEE Transactions on Image Processing*, vol. 29, pp. 8339–8354, 2020.
- [19] Stefan Van der Walt, Johannes L Schönberger, Juan Nunez-Iglesias, François Boulogne, Joshua D Warner, Neil Yager, Emmanuelle Gouillart, and Tony Yu, "scikit-image: image processing in python," *PeerJ*, vol. 2, pp. e453, 2014.
- [20] S Grace Chang, Bin Yu, and Martin Vetterli, "Adaptive wavelet thresholding for image denoising and compression," *IEEE transactions on image processing*, vol. 9, no. 9, pp. 1532–1546, 2000.
- [21] Alex Clark, "Pillow (pil fork) documentation," *Readthedocs*. <https://Buildmedia.Readthedocs.Org/Media/Pdf/Pillow/Latest/Pillow.Pdf>, 2015.